Article:
Bingham, RJ, Rizzi, LG, Cabriolu, R et al. (2013) Communication: Non-monotonic supersaturation dependence of the nucleus size of crystals with anisotropically interacting molecules. Journal of Chemical Physics, 139 (24). 241101. ISSN: 0021-9606

https://doi.org/10.1063/1.4861044

Non-monotonic supersaturation dependence of the nucleus size of crystals with anisotropically interacting molecules

R.J. Bingham,[1] L.G. Rizzi,[1] R. Cabriolu,[2] and S. Auer[1]

[1]*School of Chemistry, University of Leeds, Leeds, LS2 9JT, UK*
[2]*Dept. of Civil and Environmental Engineering, George Washington University, Washington DC, 20052, USA*

We study the nucleation of model two-dimensional crystals in order to gain insight into the effect of anisotropic interactions between molecules on the nucleation mechanism. With the aid of kinetic Monte Carlo (kMC) simulations and the forward flux sampling algorithm, we determine the growth probability $P(n)$ of a cluster of n molecules as a function of the supersaturation s. It is found that with increasing degree of interaction anisotropy the nucleus size (defined as the cluster size at which $P(n) = 0.5$) can increase with increasing s, with sharp jumps at certain s values. Analysis of the cluster shape reveals that nucleation in the system studied is of a non-standard form, in that it embodies elements of both the classical nucleation theory and the density functional theory frameworks.

PACS numbers: 81.10.Aj,87.15.A-,64.60.qe

The nucleation of crystals from molecules that interact via anisotropic potentials has been widely researched, not only because of the fundamental significance [1–5], but also due to the variety of applications, with prominent research areas including; (i) the growth of atomic metal clusters on substrates with anisotropic character [6–11], (ii) the formation of crystals by the interactions of nano-patterned materials [12–20] and (iii) the nucleation of amyloid fibrils, where the anisotropy is caused by strongly directional hydrogen bonds [21–26].

The propensity for a macroscopic crystal to nucleate can be characterized by the nucleus size, n^*, (also know as the critical nucleus size) the size a growing cluster must surpass to be more likely to grow than dissolve. According to classical nucleation theory (CNT) [27] in a single component system, there exists a well defined n^* at the cluster size which requires maximal work for its formation. Recent computational and theoretical research has shown that introducing anisotropy into the interactions between molecules creates ambiguity, changing the well defined nucleus size to a distribution of nucleus sizes [23, 24]. The resultant change to the nucleation mechanism has been shown to affect the solubility of cluster [22], crystal nucleation rate [28] and nucleation pathway [3]. Here we directly measure the distribution of nucleus sizes, characterize the dependence on the interaction anisotropy and supersaturation and relate this to the nucleus shape to explain the peculiar behavior of n^*.

Our computations use the Kossel-Stranski model, where molecules are schematized as blocks arranged in a two dimensional lattice with square symmetry [29]. The lattice is a convenience that allows the easy specification of both the cluster surface configuration and the bonding arrangements and strengths. The model also has one-to-one correspondence with the Ising model [30]. Only nearest neighbor interactions in the x and y directions are considered. The bond energies are defined by dimensionless parameters given by $\psi_i = E_i/2k_BT$ $(i = x, y)$, where E_i is the interaction energy between molecules in the x or y direction and k_B and T have their conventional meanings. We vary the strength of the interaction in the x direction while fixing $\psi_y = 1$ to study the effect of anisotropic interactions, which is characterized by the ratio $\xi = \psi_x/\psi_y$.

To investigate the response of n^* to the introduction of anisotropic interactions, we employ kinetic Monte Carlo (kMC) to simulate anisotropies $\xi = 1, 3, 5, 8$ and 10 and a range of supersaturations, s, defined by $s = \Delta\mu/k_BT$, where $\Delta\mu$ is the difference in chemical potential between the bulk old and new phases. As the simulation progresses, the number of occurrences of each cluster size is recorded in order to generate the growth probability, $P(n)$, as a function of cluster size n, given by

$$P(n) = N_{\text{macro}}/N(n), \qquad n = 2 \ldots N_{\text{macro}} \tag{1}$$

where $N(n)$ is the number of first occurrences of cluster size n and N_{macro} is the number of occurrences of the macroscopic crystal [31]. In earlier work [28], the nucleation rate was calculated by measuring the probability that a dimer will grow to macroscopic size. In order to measure the full $P(n)$ curve and hence the nucleus size at low s values, the direct forward flux sampling (FFS) algorithm is used [32]. To implement the FFS algorithm we split the range of cluster sizes n into windows of size Δn creating interfaces at $n_k = 2 + k\Delta n$, where k takes integer values. This divides the simulation into a number of shorter simulations, where N_r replicas of the system attempt to reach the interface at n_{k+1} starting from configurations with $n = n_k$. It was found that $\Delta n = 20$ and 1000 successful attempts reproduces earlier kMC results [28] while saving considerable computation time. In total, around 320 simulations were made taking N_r between 1200 and 1×10^{13} to cover different combinations of ξ and s.

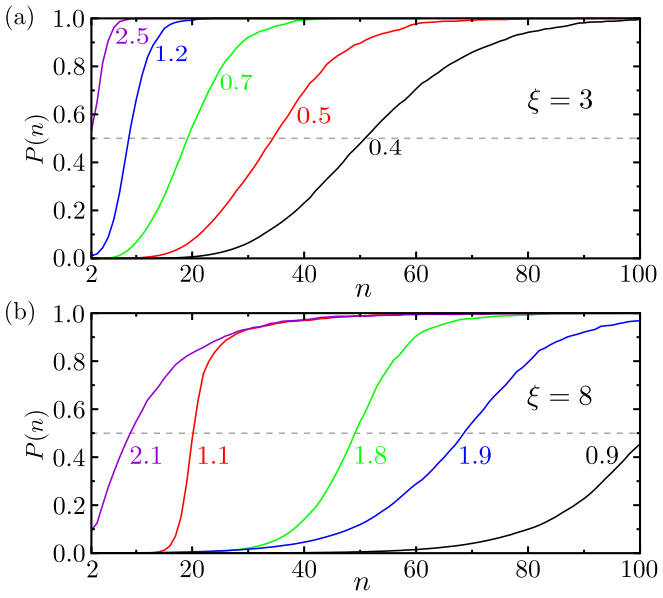

FIG. 1: (Color online) Growth probability $P(n)$ against cluster size n for anisotropies (a) $\xi = 3$ and (b) $\xi = 8$. The supersaturations are labeled within the figure. A guide for the eye is drawn at $P(n) = 0.5$, the probability that defines n^*. The trend in $P(n)$ with changes in supersaturation becomes less predictable as the anisotropy increases.

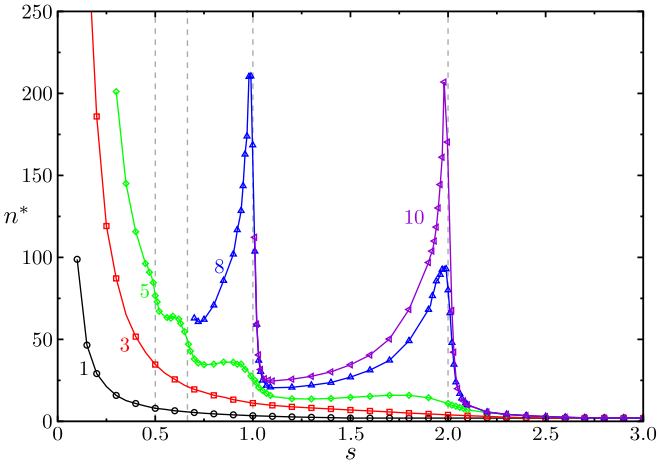

FIG. 2: (Color online) Nucleus size n^* against the supersaturation s, for various interaction anisotropies. As the anisotropy is increased the decay in n^* becomes non-monotonic, in contrast to the predictions of CNT. The dotted lines represent 'transition' supersaturations, as predicted by the theory of Kashchiev *et al.* [22, 24] at $s = 2, 1, 2/3, 1/2$.

Figure 1 shows representative $P(n)$ curves for two anisotropies and various supersaturations. For anisotropy $\xi = 3$ (Fig. 1(a)) the probabilities $P(n)$ have similar behavior to the isotropic ($\xi = 1$) case, in which reducing the supersaturation shifts the curve to the right and increases the width. At higher anisotropy $\xi = 8$ (Fig. 1(b)) the $P(n)$ curves no longer show a consistent trend instead 'jumping' as supersaturation is lowered. All the $P(n)$ curves show logistic-type growth but at higher anisotropy the change in shape with variation in s appears less uniform.

A broader view of the changes in nucleation probability is required, so we use the growth probability $P(n)$ to calculate the nucleus size n^*, commonly defined as the cluster size at which $P(n) = 0.5$. Figure 2 shows the supersaturation dependence of the nucleus size n^*. At low anisotropies ($\xi = 1, 3$) n^* decays monotonically with s as predicted by CNT, however at higher anisotropy ($\xi = 5, 8, 10$) the decay becomes non-monotonic, n^* displaying peaks at 'transition' s values above which the nucleus size shows a dramatic decline. This peculiar behavior is a departure from the classical behavior predicted by CNT. The transition values correspond with those predicted by Kashchiev *et al.* [22, 24] for jumps in the solubility of amyloid fibril, where each supersaturation region is defined by the number of rows a cluster requires in order to grow irreversibly. A general formula for the transition supersaturations can be derived [22]; $S_i = 2\psi_y/i$ where i is the number of rows in a cluster, a row being defined as growth in the strong bonding direction, x. Above each S_i a cluster with i rows can grow irreversibly, hence above $S_1 = 2\psi_y/1 = 2$ all clusters with one row can grow to macroscopic size, which defines this region as the metanucleation range, where each single molecule acts as a nucleus and hence nucleation is instantaneous. This is independent of anisotropy, as reflected in Fig. 2, where all anisotropies have very small nucleus sizes $s > 2$. If $1 < s < 2$ a cluster needs two rows to grow to macroscopic size, therefore the nucleus must consist of one row, with an additional molecule starting a new row. The appearance of a second row can occur at a variety of lengths of the initial row, which leads to a distribution of nucleus sizes. Similarly when $2/3 < s < 1$ a three row cluster is required, hence the nucleus is two rows with an additional molecule starting a third row. Each descending supersaturation interval adds an additional row to this requirement. A similar nucleation mechanism has recently been observed in oligomer formation experiments of amyloid fibrils [33].

Based on the correspondence between our results and the theoretical model [24], additional simulations were performed to investigate the causes of the non-monotonic decay in n^* vs s. The shape of the cluster was recorded and analyzed at each size n for different combinations of s and ξ and again averages and distributions were evaluated using 1000 completed trajectories. Fig. 3(a) shows the average number of rows in a cluster, $\langle i \rangle$, against the cluster size n. While the anisotropy is varied from $\xi = 1$ to 8, the supersaturation is held fixed at $s = 1.7$, a point where there is significant variation in n^* with changes in ξ. For $\xi = 1$ and 3 the average number of rows grows unbounded but at higher anisotropy ($\xi = 5$ and 8) the rate

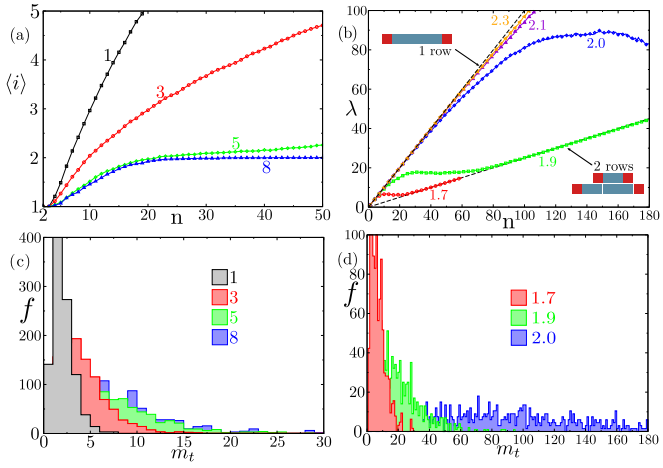

FIG. 3: (Color online) (a) The average number of rows $\langle i \rangle$ in a cluster against cluster size n for various anisotropies. The supersaturation is held fixed at $s = 1.7$. A row is defined as molecules aligned along the strong bonding direction. (b) The shape factor λ against cluster size n at various supersaturations. The anisotropy is now fixed at $\xi = 8$. Lines are added to indicate the shape factors of ideal one-row and two-row clusters. (c) Histogram of the transition size m_t of the nuclei, from the same data used to generate (a). The transition size is the length of the first row upon formation of the second row. (d) Histogram of the transition size m_t of the nuclei, using the same data used to generate (b).

of row increase has dramatically slowed and has stopped at $\langle i \rangle = 2$ when $\xi = 8$, indicating that the clusters are elongated and in agreement with the model [24].

To quantify the shape of the clusters during the nucleation process, the shape factor $\lambda = n/i^2$, is introduced. Greater λ values correspond to elongated cluster shapes. Fig. 3(b) shows how the shape factor reflects the changing shape of a nucleating cluster, where the anisotropy is fixed at $\xi = 8$ and the supersaturation is varied. In the metanucleation region ($s > 2$), $\lambda = n$ and the cluster appears as a single row, adding molecules at the cluster ends. For supersaturations below the nucleation/metanucleation boundary, $s < 2$, λ initially increases rapidly before transitioning to a slower, but still linear rate of increase, which illustrates that the cluster initially grows as a single row, before transforming to a two row cluster. The cluster size at which λ passes through a stationary point before settling on the line indicating a two row cluster increases as $s \to 2$ which results in both the increase and the peak in n^* seen in Fig. 2.

In order to determine the distribution of nucleus sizes we record in histograms the frequency f of transition sizes m_t, defined by the length of the first row upon formation of the second row. First we held the supersaturation fixed at $s = 1.7$ and, as shown in Fig. 3(c), the mean transition size and the width of the distribution increases as the anisotropy is increased. As shown above, in this supersaturation range ($1 < s < 2$) a nucleus consists of a single row with an additional molecule in a second row, hence measuring the transition size is in effect measuring the size at which a cluster becomes a nucleus. Now we consider the distribution of frequencies of m_t across the transition between different supersaturations ranges. Figure 3(d) records the frequency of transition sizes m_t using the same data as Fig 3(b). The transition sizes reflect the trend in n^* shown in Fig. 2 as the mean value of the frequency distributions of m_t increase as s increases. At $s = 1.7$ the maximum m_t occurs at ~ 20 molecules, which correlates with the cluster size at which the $\xi = 8$ curve in Fig. 3(a) reaches its maximum value $\langle i \rangle = 2$. When the supersaturation is increased to $s = 1.9$ the tail of the distribution has increased, until at $s = 2.0$ where the distribution appears flat across the range of transitions sizes from $m_t = 1$ to 180. The nucleating clusters at $s = 2.1, 2.3$ very rarely undergo a transition to a two row cluster (as seen in Fig. 3(b)) and therefore do not appear in this plot.

The observed behavior of n^* can be rationalized within the context of the stochastic growth modeled by our simulations, where the likelihood of molecule addition depends upon the relative changes in the nucleation work. Adding a molecule in the x direction, creating two broken weak bonds in the y direction costs $2\psi_y - s$, while creating a new row by adding a molecule in the y direction creates two broken strong bonds, which costs $2\psi_x - s$. This energy cost increases with the anisotropy ratio ξ. When these terms are comparable at low anisotropy, the cluster is likely to grow in an isotropic fashion. At high ξ, the barrier to creating new rows is higher, so the cluster is more likely to have reached large row lengths before reaching the number of rows required to grow irreversibly. This is reflected in both the widening m_t distributions (Fig. 3(c)) and the subsequent increase in n^* (Fig. 2) with increases in ξ. As $s \to S_1 = 2$ the work $(2\psi_y - s)$ to extend a single row tends to zero, hence the transition size will increase, as seen in Fig. 3(d) and this results in the peaks in n^* as $s \to 2$. When $s < S_2 = 1$ a three row cluster is required for irreversible growth, but as $s \to 1$ the work to extend a two row cluster tends to zero and hence similar peaks in n^* are observed. Similar relationships can be shown for all supersaturation regions.

In summary, the presented analysis of the nucleus shape and dependence on s and ξ reveals a clear picture of the nucleation mechanism of crystals with anisotropic molecular interactions. As the anisotropy is increased the classical description (as used in CNT) breaks down because the concept of a well-defined nucleus no longer exists. From our shape analysis we find that; (i) At high anisotropy the number of rows in a cluster saturates at the height of a nucleus. (ii) The formation of the row that achieves the nucleus height can occur at a range of transition sizes, that increases both as ξ is increased and as a transition supersaturation S_i is approached from below. (iii) The broadening range of transition sizes coupled

with requirement of a minimum nucleus height leads to a wide variety of nuclei, ultimately causing the peculiar behavior seen in the s dependence of n^*. It should be noted however that the peaks in n^* at S_i resemble those of the critical nucleus radius against system composition seen in the density functional theory (DFT) description of nucleation [34]. The DFT model describes nucleation in a two-component continuous fluid, where as the difference in composition approaches the spinodal value, the critical nucleus radius tends to infinity, against the predictions of classical theory. In our system the transition supersaturations S_i are spinodal values for the extension of existing cluster rows, reinforcing this commonality. Nucleation of crystals from molecules with anisotropic interactions can therefore be seen to be a non-standard form of nucleation, in that it displays decrease of n^* with s of CNT and the asymptotic spinodal $n^*(s)$ behavior seen in DFT, but cannot be entirely characterized by either of these frameworks.

The subtleties of nucleation from anisotropically interacting molecules has implications for both practical and theoretical studies. In kinetic studies of amyloid fibrillation, the nucleus size is assumed to be a constant for use as a parameter in rate equations [35]. We have shown that this assumption is problematic, that in fact a wide distribution of nucleus sizes are possible, especially near transition supersaturations, where additional conformational factors could also play a role. In the experimental studies of nucleation of amyloid fibrils, the anisotropy arises from the disparity in bonding strengths between neighboring peptides within each β sheet and those in neighboring β sheets, which could be tuned by changing the amino acid sequence within the peptides allowing for the control of the fibril nucleus size and the macroscopic fibril morphology.

The authors would like to thank Professor Dimo Kashchiev and Professor Pietro Ballone for helpful comments on the manuscript. This work was supported by the Leverhulme Trust (RJB) and a CNPq grant No. 245412/2012-3 (LGR).

[1] K. Van Workum and J. F. Douglas, Phys. Rev. E **73**, 031502 (2006).
[2] S. C. Glotzer and M. J. Solomon, Nature Mater. **6**, 557 (2007).
[3] S. Whitelam, J. Chem. Phys. **132**, 194901 (2010).
[4] L. G. López, D. H. Linares, A. J. Ramirez-Pastor, and S. A. Cannas, J. Chem. Phys. **133**, 134706 (2010).
[5] P. Yi and G. C. Rutledge, Annu. Rev. Chem. Biomol. Eng. **3**, 157 (2012).
[6] E. Hahn, E. Kampshoff, A. Fricke, J.-P. Bucher, and K. Kern, Surf. Sci. **319**, 277 (1994).
[7] C. Mottet, R. Ferrando, F. Hontinfinde, and A. C. Levi, Surf. Sci. **417**, 220 (1998).
[8] R. Ferrando, F. Hontinfinde, and A. C. Levi, Surf. Sci. **402**, 286 (1998).
[9] S. Rusponi, C. Boragno, R. Ferrando, F. Hontinfinde, and U. Valbusa, Surf. Sci. **440**, 451 (1999).
[10] A. Videcoq, F. Hontinfinde, and R. Ferrando, Surf. Sci. **515**, 575 (2002).
[11] Y. Xia, Y. Xiong, B. Lim, and S. E. Skrabalak, Angew. Chem. Int. Ed. **48**, 60 (2009).
[12] A. Yethiraj and A. van Blaaderen, Nature **421**, 513 (2003).
[13] E. Bianchi, J. Largo, P. Tartaglia, E. Zaccarelli, and F. Sciortino, Phys. Rev. Lett. **97**, 168301 (2006).
[14] E. G. Noya, C. Vega, J. P. K. Doye, and A. A. Louis, J. Chem. Phys. **127**, 054501 (2007).
[15] R. Prieler, J. Hubert, D. Li, B. Verleye, R. Haberkern, and H. Emmerich, J. Phys. Condens Matter **21**, 464110 (2009).
[16] M. R. Jones, R. J. Macfarlane, B. Lee, J. Zhang, K. L. Young, A. J. Senesi, and C. A. Mirkin, Nature Mater. **9**, 913 (2010).
[17] F. Romano and F. Sciortino, Soft Matter **7**, 5799 (2011).
[18] S. Sacanna and D. J. Pine, Curr. Opin. Colloid Interface Sci. **16**, 96 (2011).
[19] F. J. Martinez-Veracoechea, B. M. Mladek, A. V. Tkachenko, and D. Frenkel, Phys. Rev. Lett. **107**, 045902 (2011).
[20] F. Smallenburg and F. Sciortino, Nature Phys. (2013).
[21] H. J. Kwon, Y. Tanaka, A. Kakugo, K. Shikinaka, H. Furukawa, Y. Osada, and J. P. Gong, Biochemistry **45**, 10313 (2006).
[22] D. Kashchiev and S. Auer, J. Chem. Phys. **132**, 215101 (2010).
[23] R. Cabriolu, D. Kashchiev, and S. Auer, J. Chem. Phys. **133**, 225101 (2010).
[24] D. Kashchiev, R. Cabriolu, and S. Auer, J. Am. Chem. Soc. **135**, 1531 (2013).
[25] A. Irbäck, N. Linnemann, B. Linse, S. Wallin, et al., Phys. Rev. Lett. **110**, 058101 (2013).
[26] R. Ni, S. Abeln, M. Schor, M. A. C. Stuart, and P. G. Bolhuis, Phys. Rev. Lett. **111**, 058101 (2013).
[27] D. Kashchiev, *Nucleation: Basic theory with applications* (Butterworth-Heinemann (Boston), 2000).
[28] R. Cabriolu, D. Kashchiev, and S. Auer, J. Chem. Phys. **137**, 204903 (2012).
[29] I. N. Stranski and R. Kaischew, Z. Phys. Chem. Abt. B **26**, 100 (1934).
[30] V. A. Shneidman, K. A. Jackson, and K. M. Beatty, J. Chem. Phys. **111**, 6932 (1999).
[31] J. H. Ter Horst and D. Kashchiev, J. Chem. Phys. **119**, 2241 (2003).
[32] R. J. Allen, C. Valeriani, and P. R. ten Wolde, J. Phys. Condens. Matter **21**, 463102 (2009).
[33] L. Young, H. Ndlovu, T. W. Knapman, S. A. Harris, S. E. Radford, and A. E. Ashcroft, Int. J. Ion Mobil. Spectrom. **16**, 29 (2013).
[34] J. W. Cahn and J. E. Hilliard, J. Chem. Phys. **31**, 688 (1959).
[35] S. I. A. Cohen, M. Vendruscolo, C. M. Dobson, and T. P. J. Knowles, J. Mol. Biol. **421**, 160 (2012).